Experimental ladder proof of Hardy's nonlocality for high-dimensional quantum systems

Lixiang Chen,[1,*] Wuhong Zhang,[1] Ziwen Wu,[1] Jikang Wang,[1] Robert Fickler,[2] and Ebrahim Karimi[2,†]

[1]*Department of Physics and Collaborative Innovation Center for Optoelectronic Semiconductors and Efficient Devices, Xiamen University, Xiamen 361005, China*

[2]*Department of Physics, University of Ottawa, 25 Templeton Street, Ottawa, Ontario, Canada K1N 6N5*

(Received 5 September 2016; revised manuscript received 4 January 2017; published 9 August 2017)

Recent years have witnessed a rapidly growing interest in high-dimensional quantum entanglement for fundamental studies as well as towards novel applications. Therefore, the ability to verify entanglement between physical qudits, d-dimensional quantum systems, is of crucial importance. To show nonclassicality, Hardy's paradox represents "the best version of Bell's theorem" without using inequalities. However, so far it has only been tested experimentally for bidimensional vector spaces. Here, we formulate a theoretical framework to demonstrate the ladder proof of Hardy's paradox for arbitrary high-dimensional systems. Furthermore, we experimentally demonstrate the ladder proof by taking advantage of the orbital angular momentum of high-dimensionally entangled photon pairs. We perform the ladder proof of Hardy's paradox for dimensions 3 and 4, both with the ladder up to the third step. Our paper paves the way towards a deeper understanding of the nature of high-dimensionally entangled quantum states and may find applications in quantum information science.

DOI: 10.1103/PhysRevA.96.022115

I. INTRODUCTION

In 1935, Einstein, Podolsky, and Rosen (EPR) published the famous EPR paradox, which questioned the completeness of quantum mechanics and has led to massive investigations into the concept of quantum entanglement [1]. In 1964, Bell proved that the EPR argument invoking local realism leads to algebraic predictions that are in contradiction to quantum mechanics, which found its mathematical expression in the so-called Bell inequality [2]. Since then, many interesting experiments have tested the Bell inequalities, leading to a very strong agreement with quantum mechanics while disfavoring hidden variable theories [3]. Thirty years later, Hardy formulated another paradox challenging the idea of locality and hidden variables [4,5]. In contrast to Bell's inequality, Hardy's theory is an attempt to demonstrate nonlocality without inequalities, and, as such, Mermin referred to it as "the best version of Bell's theorem" [6]. In Hardy's original theory, the nonlocality proof was shown with the use of two spin-half particles [4,7–9]. Hardy's idea has so far been realized experimentally using entangled qubits, two-level quantum states, implemented by the polarization, energy time, and orbital angular momentum (OAM) of photons [10–13]. A significant progress has been made by Boschi *et al.* [14] and Barbieri *et al.* [15], who generalized Hardy's proof to a ladder version that enabled the significant increase of probability of the nonlocal events.

In the above-mentioned experimental realization analogous to spin-half particles, only vector spaces of dimension 2 (qubits) were considered. However, from both the fundamental and applied points of view, entangling systems in higher-dimensional states (qudits) are of considerable importance, as they offer higher information-density coding, increased level of security, and new quantum imaging techniques [16–20]. Recent theoretical efforts were made to generalize Hardy's argument into a high-dimensional scenario, where two spin-s particles were involved. This can be traced back to the original proposal by Clifton and Niemann [21]. Kunkri and Choudhary then provided a more compact logic structure of the nonlocality condition for two spin-s particles [22]. It was first conjectured by Ghosh and Kar [23] and Seshadreesan and Ghosh [24], and proven by Rabelo *et al.*, that there existed a bounded violation of locality constraints allowed by the quantum formalism, with the maximum Hardy probability equal to $p_H = (5\sqrt{5} - 11)/2$ [25]. More importantly, the generalization to high-dimensional systems is of particular interest because it brings Hardy's paradox closer to the original EPR scenario, where the measurements have an arbitrarily large number of outcomes [26]. Additionally, Cabello first theoretically considered the ladder proof of Bell's theorem for any maximally entangled states of two spin-s particles [27]. However, these theoretical schemes for high-dimensional systems have not yet been translated into experimental implementations. Additionally, the photon's OAM degree of freedom, which can be exploited to construct an inherently high-dimensional Hilbert space [28,29], has only been used for a two-dimensional test, and thus has not yet been fully explored in the framework of Hardy's paradox. Here, we employ OAM of entangled photons to mimic a high spin-s system, and demonstrate theoretically and experimentally the ladder proof in high-dimensional OAM subspaces of $d = 3,4$ with the ladder order up to $K = 3$. We thus demonstrate that quantum mechanics is in contradiction with the existence of local hidden variable theories.

II. THEORETICAL FORMULATION

In the original proposals [21–24], spin particles were considered to simulate high-dimensional quantum systems. For spin-s particles, quantum mechanics states that the component of a spin measured along the z axis can only take the values $S_z = s_z\hbar$, where $s_z = -s, -(s-1), \ldots, s-1, s$ and $\hbar$ is the reduced Planck's constant [30]. For example, for a spin-1 particle, the possible values are $s_z = -1,0,+1$. Thus, it allows the construction of a high-dimensional Hilbert space that is spanned by a standard orthonormal basis ordered by s_z denoted as $|s_z\rangle$. Unlike the polarization degree of freedom

*Corresponding authors: chenlx@xmu.edu.cn
†ekarimi@uottawa.ca

 ©2017 American Physical Society

of photons, which describes the vectorial nature of light and is only associated with a two-dimensional space, OAM is related to the helical phase structure. If light exhibits an azimuthal phase structure such as $\exp(i\ell\phi)$, each photon carries a well-defined OAM of $\ell\hbar$. Here, ϕ is the azimuthal angle of polar coordinates, and ℓ is an integer value describing the OAM quantum number [31]. As ℓ is theoretically unbounded, the OAM degree of photons can be used as a physical realization of qudits in a high-dimensional Hilbert space [32], similar to a high-dimensional spin space of particles described above. The use of OAM as another degree of freedom to test Hardy's paradox has two major advantages over the analogous cases with high spin values: First, photonic OAM, as well as arbitrary superpositions thereof, can be readily generated and conveniently measured based on the use of a commercial spatial light modulator (SLM) [33]. Second, Hardy's proof requires high-dimensional bipartite states that are nonmaximally entangled, which is well realized for the two-photon OAM states generated by spontaneous parametric down conversion (SPDC) [34]. Since both key features are extremely hard to implement or even nonexistent for higher spins, high-dimensionally entangled OAM quanta of photon pairs provide an ideal playground for an experimental verification of Hardy's paradox.

Let us first formulate a ladder set of conflicting classical logic statements in the high-dimensional spin-s subspaces. Assume $A_0, A_1, \ldots,$ and A_K are $K+1$ different noncommuting spin observables for particle A, and similarly $B_0, B_1, \ldots,$ and B_K are those for particle B. The measurement outcomes for A_k and B_l $(k,l = 0,1,\ldots,K)$ range from $-s$ to $+s$, totally including $d = 2s + 1$ discrete values. With $P(A_k = i, B_l = j)$ as the joint probability of obtaining $A_k = i$ and $B_l = j$, we assume the following set of zero probabilities:

$$P(A_0 = s, B_0 = s) = 0, \tag{1}$$

$$P(A_k = s, B_{k-1} = i) = 0 \quad \text{for} \quad i = s-1, s-2, \ldots, -s-1, -s, \tag{2}$$

$$P(A_{k-1} = j, B_k = s) = 0, \quad \text{for} \quad j = s-1, s-2, \ldots, -s-1, -s, \tag{3}$$

where k ranges from 1 to K. Equations (1)–(3) consist of a total of $4Ks + 1$ equations. In any local hidden variable theory, according to Eqs. (1)–(3), we should also obtain a zero probability for all $A_K = s$ and $B_K = s$, i.e., $P(A_K = s, B_K = s) = 0$. However, quantum mechanics allows a suitable choice of observables to make the Hardy fraction,

$$P(A_K = s, B_K = s) > 0, \tag{4}$$

which is logically inconsistent with the classical predictions. By using reduction to absurdity, we show the basic idea of the high-order ladder proof in the diagram of Fig. 1, where, without loss of generality, $K = 2$ for a three-dimensional case ($s = 1, d = 3$) is illustrated. Note that our formalism includes the already known special cases: For $K = 1$, Eqs. (1)–(4) reduce to those of the original proposal of Hardy's test with spin-s systems that only considered a single step [22–24]; for $s = 1/2$, they reduce to the ladder proof of Hardy's nonlocality with two-level quantum systems [11–14].

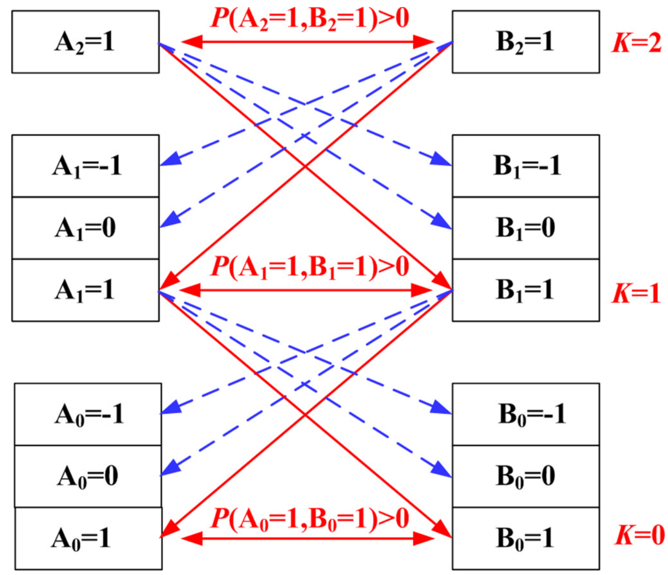

FIG. 1. The diagram of Hardy's ladder proof with $K = 2$ in three-dimensional OAM subspace. Blue (dash) lines indicates zero probabilities while red (solid) lines corresponds to nonzero probabilities. According to the local hidden variable theory, we know that once we measured $P(A_2 = 1, B_2 = 1) > 0$ then both $P(A_2 = 1, B_1 =) = 0$ and $P(A_2 = 1, B_1 = 0) = 0$ will lead to $P(A_2 = 1, B_1 = 1) > 0$. Similarly, we also have $P(A_1 = 1, B_2 = 1) > 0$. Thus we have $P(A_1 = 1, B_1 = 1) > 0$. We repeat this to go down the ladder and finally obtain $P(A_0 = 1, B_0 = 1) > 0$, being inconsistent with Eq. (1) of $P(A_0 = 1, B_0 = 1) = 0$. In other words, if the assumptions of Eqs. (1)–(3) hold, the measurement result of $P(A_2 = 1, B_2 = 1) > 0$ will support quantum mechanics but contradict any local hidden variable theory.

The first key step to transport the conceptual idea to experimentally implementable states is to define a secession of suitable observables, A_k and B_l, that satisfy the logical statements of Eqs. (1)–(4). For Hardy's test in two-dimensional spaces, such as for spin-1/2 particles or photon polarizations, the observables are readily defined by 2×2 unitary matrices, the general form of which reads [5,10–14]

$$M_k^{(2)} = \begin{bmatrix} \cos\theta_k & e^{i\xi_k}\sin\theta_k \\ e^{-i\xi_k}\sin\theta_k & -\cos\theta_k \end{bmatrix}. \tag{5}$$

For each k, the matrix $M_k^{(2)}$ defines a pair of orthogonal states. Similarly, we can construct the high-order matrix $M_k^{(2s+1)}$, which defines $2s+1$ orthogonal states in the high-dimensional spin-s space. We start with $s = 1$, i.e., three-dimensional states or qutrits, for which we construct $M_k^{(3)}$ by analogy with the eigenvectors in a uniaxial crystal [35]. Light propagates in a uniaxial crystal with its wave vector specified by $\hat{\mathbf{k}} = (\cos\theta, \sin\theta\cos\varphi, \sin\theta\sin\varphi)$, where θ and φ are the polar and azimuthal angles, respectively. Then two eigenvectors of o-ray and e-ray are given by $\hat{\mathbf{o}} = (0, \sin\varphi, -\cos\varphi)$ and $\hat{\mathbf{e}} = (\sin\theta, -\cos\theta\cos\varphi, -\cos\theta\sin\varphi)$, respectively [36]. These $\hat{\mathbf{k}}$, $\hat{\mathbf{o}}$, and $\hat{\mathbf{e}}$ form a set of mutually orthogonal unit vectors, based on which we can construct a unitary matrix as follows:

$$M_k^{(3)} = \begin{bmatrix} \cos\theta_k & e^{i\xi_k}\sin\theta_k\cos\varphi_k & e^{i(\xi_k+\eta_k)}\sin\theta_k\sin\varphi_k \\ 0 & e^{-i\eta_k}\sin\varphi_k & -\cos\varphi_k \\ e^{-i\xi_k}\sin\theta_k & -\cos\theta_k\cos\varphi_k & -e^{i\eta_k}\cos\theta_k\sin\varphi_k \end{bmatrix}, \tag{6}$$

where $e^{i\xi_k}$ and $e^{i\eta_k}$ as well as their conjugates are introduced to generalize the Euclidean space spanned by the real vectors of $\hat{\mathbf{k}}$, $\hat{\mathbf{o}}$, and $\hat{\mathbf{e}}$ to the associated Hilbert space.

We employ the OAM entangled photon pairs generated by SPDC for our ladder test of Hardy's paradox. The two-photon wave function can be written as $|\Psi\rangle_{\rm SPDC} = \sum_\ell C_\ell |\ell\rangle_A |-\ell\rangle_B$, where C_ℓ denotes the amplitude probability of finding one signal photon (index A) with $\ell\hbar$ OAM and its partner idler photon (index B) with $-\ell\hbar$ [37]. To mimic spin-1 particles, we restrict our measurements to a subset including three OAM eigenstates such that the entangled state reads as $|\Psi\rangle_{\rm 3D} = C_l|l\rangle_A|-l\rangle_B + C_m|m\rangle_A|-m\rangle_B + C_n|n\rangle_A|-n\rangle_B$. Based on Eq. (6), we define the OAM measurement basis for the signal and idler photon, respectively, in terms of OAM eigenstates as

$$\begin{bmatrix} |A_k=+1\rangle \\ |A_k=0\rangle \\ |A_k=-1\rangle \end{bmatrix} = M_k^{(3)} \begin{bmatrix} |l\rangle_A \\ |m\rangle_A \\ |n\rangle_A \end{bmatrix}, \tag{7}$$

$$\begin{bmatrix} |B_k=+1\rangle \\ |B_k=0\rangle \\ |B_k=-1\rangle \end{bmatrix} = M_k^{(3)} \begin{bmatrix} |-l\rangle_B \\ |-m\rangle_B \\ |-n\rangle_B \end{bmatrix}. \tag{8}$$

We have calculated and specified the exact parameters θ_k, φ_k, ξ_k, and η_k (Table S1 of Ref. [38]). By substituting Eqs. (7) and (8) into Eqs. (2) and (3), and after a lengthy yet straightforward algebra, we calculate analytically the K-order Hardy fractions of Eq. (4) as

$$P_K^{(3)} = \left| \frac{C_l C_m C_n \left[C_n^{2K-1}\left(C_l^{2K} - C_m^{2K}\right)\cos^2\varphi_0 + C_m^{2K-1}\left(C_l^{2K} - C_n^{2K}\right)\sin^2\varphi_0\right]}{C_m^{2K}\left(C_l^{2K+1} + C_n^{2K+1}\right)\sin^2\varphi_0 + C_n^{2K}\left(C_l^{2K+1} + C_m^{2K+1}\right)\cos^2\varphi_0} \right|^2. \tag{9}$$

One can see that the Hardy fractions have a dependence on the entangled spiral spectrum characterized by C_l, C_m, and C_n. Note that Hardy's test still becomes invalid for maximal OAM entanglement with $C_l = C_m = C_n$. Additionally, if $\varphi_0 = 0$, then P_K simply reduces to the qubit case [14], as the rank of the matrix $M_k^{(3)}$ degrades to 2 so that it explores only a two-dimensional subspace.

In an analogous way, we can continue and generalize the unitary matrix $M_k^{(3)}$ to $M_k^{(4)}$ for spin-3/2 quantum systems or equivalently to a four-dimensional OAM subspace. The set of mutually orthogonal unit vectors now reads

$$M_k^{(4)} = \begin{bmatrix} \cos\theta_k & e^{i\xi_k}\sin\theta_k\cos\varphi_k & e^{i(\xi_k+\eta_k)}\sin\theta_k\sin\varphi_k\cos\sigma_k & e^{i(\xi_k+\eta_k+\tau_k)}\sin\theta_k\sin\varphi_k\sin\sigma_k \\ 0 & 0 & e^{-i\tau_k}\sin\sigma_k & -\cos\sigma_k \\ 0 & e^{-i\eta_k}\sin\varphi_k & -\cos\varphi_k\cos\sigma_k & -e^{-i\tau_k}\cos\varphi_k\sin\sigma_k \\ e^{-i\xi_k}\sin\theta_k & -\cos\theta_k\cos\varphi_k & -e^{i\eta_k}\cos\theta_k\sin\varphi_k\cos\sigma_k & -e^{i(\eta_k+\tau_k)}\cos\theta_k\sin\varphi_k\sin\sigma_k \end{bmatrix}. \tag{10}$$

The four-dimensionally entangled two-photon state in the OAM bases can be written correspondingly as $|\Psi\rangle_{\rm 4D} = C_j|j\rangle_A|-j\rangle_B + C_l|l\rangle_A|-l\rangle_B + C_m|m\rangle_A|-m\rangle_B + C_n|n\rangle_A|-n\rangle_B$ and the desired projective measurements performed jointly on the signal and idler photons are defined as follows:

$$\begin{bmatrix} |A_k=+3/2\rangle \\ |A_k=+1/2\rangle \\ |A_k=-1/2\rangle \\ |A_k=-3/2\rangle \end{bmatrix} = M_k^{(4)} \begin{bmatrix} |j\rangle_A \\ |l\rangle_A \\ |m\rangle_A \\ |n\rangle_A \end{bmatrix}, \tag{11}$$

$$\begin{bmatrix} |B_k=+3/2\rangle \\ |B_k=+1/2\rangle \\ |B_k=-1/2\rangle \\ |B_k=-3/2\rangle \end{bmatrix} = M_k^{(4)} \begin{bmatrix} |-j\rangle_B \\ |-l\rangle_B \\ |-m\rangle_B \\ |-n\rangle_B \end{bmatrix}. \tag{12}$$

We can still calculate the desired parameters of θ_k, φ_k, σ_k and ξ_k, η_k, τ_k (Table S2 of Ref. [38]). After some algebra, we can also obtain the Hardy fraction:

$$P_K^{(4)} = |C_j\cos^2\theta_K - C_l\sin^2\theta_K\cos^2\varphi_K - C_m\sin^2\theta_K\sin^2\varphi_K\cos^2 \times \sigma_K - C_n\sin^2\theta_K\sin^2\varphi_K\sin^2\sigma_K|^2. \tag{13}$$

Along this line, we are able to theoretically construct the matrix $M_k^{(d)}$ with $d = 2s+1$ for an arbitrary s, which is the key point to realize the ladder proof of Hardy's paradox in any Hilbert space of arbitrary dimension. As an example, without loss of generality, we explicitly show the general forms of $M_k^{(5)}$ and $M_k^{(6)}$ [Eqs. (S2) and (S9) of Ref. [38]].

III. EXPERIMENTAL SETUP

We prepare the high-dimensional two-photon OAM entangled states via degenerate SPDC, where both photons have opposite OAM quanta due to angular momentum conservation [37]. A schematic overview of our optical setup is shown in Fig. 2 and experimental details can be found in the corresponding figure caption. In the experiment, we first characterize our generated entangled state, by measuring the two-photon correlated OAM spectrum. We do so by implementing a mode filter consisting of a computer-controlled phase-only SLM and a single mode fiber (SMF). We use the SLM to flatten the phase structure of a specific spatial mode, which couples efficiently into the SMF. Other modes, which are not phase flattened by the SLM, do not couple into the SMF; hence, they are filtered out. The measured normalized coincidence counts between

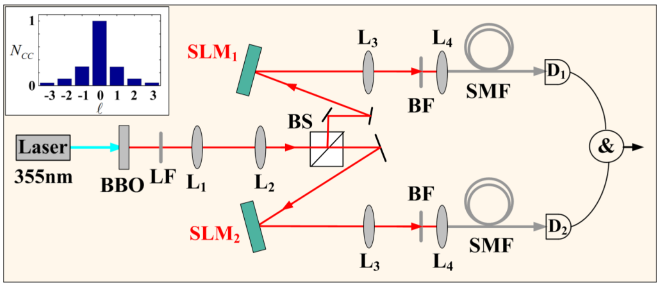

FIG. 2. Optical system for the ladder test of Hardy's paradox based on high-dimensional entangled photons. A collimated 355-nm ultraviolet laser (JDSU) pumps a 5-mm-long β-barium borate (BBO) crystal, where a degenerate 710-nm signal and idler photons are produced in pairs via type-I collinear SPDC. Afterwards, we separate the two photons into two different paths by a nonpolarizing beam splitter (BS). A longpass filter (LF) is used to block the pump beam after the crystal. The output facet of the crystal is imaged onto both spatial light modulators (SLM_1, SLM_2, Hamamatsu, X10486-1) by two lenses in a 4-f configuration ($f_1 = 200$ mm, $f_2 = 400$ mm). Each SLM is then similarly reimaged by another pair of lenses L_3 and L_4 ($f_3 = 500$ mm and $f_4 = 2$ mm) onto a single-mode fiber (SMF), which is connected to a single-photon detector (SPCM-AQRH-14). The SLM together with the SMF acts as a programmable mode filter. Bandpass filters (BF) of 10-nm width and centered at 710 nm are placed in front of SMFs to ensure degeneracy of the detected photon pairs. The detectors are connected to a coincidence counting circuit (&) with a 25-ns coincidence time window. The measured entangled OAM spectrum characterized by the peak-normalized coincidence counts N_{CC} is shown by the inset.

photons found with the OAM state of $|\ell\rangle$ in the signal arm and $|-\ell\rangle$ in the idler arm (ℓ ranging from -3 to $+3$) directly correspond to the two-photon correlated OAM spectrum. This so-called spiral spectrum is shown in the inset of Fig. 2. The limited bandwidth, and hence the nonmaximal entanglement, can be clearly seen, as the coincidence rate decreases with increasing ℓ values.

In order to perform Hardy's test, we need to measure a sequence of OAM superposition states. As before, we use the SLMs in combination with the SMF to project onto the required modes. For example, if we want to measure the joint probability of $P(A_k = +s, B_{k-1} = i)$, we program the SLM to project the signal and idler photons onto the states of $|A_k = +s\rangle$ and $|B_{k-1} = i\rangle$, respectively. These states correspond to superpositions of OAM eigenstates, as defined by Eqs. (7) and (8), or Eqs. (11) and (12). We summarize the mathematical principle of preparing the desired holograms [Eq. (S1) of Ref. [38]].

IV. EXPERIMENTAL RESULTS

Without loss of generality, we restrict our first set of measurements to a three-dimensional OAM subspace of $l = -1,0,+1$. From the measured spiral spectrum (see Fig. 2 inset) we calculate the normalized coefficients of C_ℓ, which leads to the nonmaximally entangled state $|\Psi\rangle_{3D} = 0.795|0\rangle_A|0\rangle_B + 0.431|+1\rangle_A|-1\rangle_B + 0.428|-1\rangle_A|+1\rangle_B$, with the reasonable assumption of C_ℓ being real-valued [39]. In our first demonstration, we consider a ladder scenario with $K = 3$. Based on Eq. (9), we can predict the quantum-mechanically expected Hardy fractions as $P_1 = 6.89\%$, $P_2 = 14.12\%$, and $P_3 = 17.11\%$, respectively. Note that the desired joint measurements are specified by the parameters of θ_k and φ_k in $M_k^{(3)}$ (Table S1 of Ref. [38]). In the experiment, we first start with measuring the joint probabilities defined in Eqs. (1)–(3) by performing in total $4Ks + 1 = 13$ ($K = 3, s = 1$) projective measurements on the OAM superpositions for both photons. For all, we expect a joint probability of exactly zero. As can be seen in Fig. 3, they are very small; however, due to experimental imperfections, such as slight misalignments or nonperfect

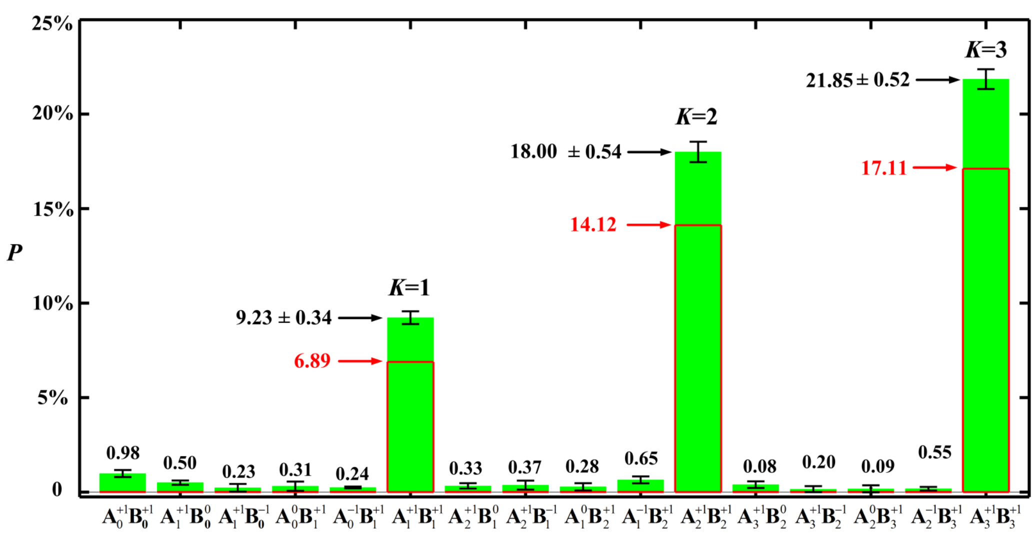

FIG. 3. Experimental results for the ladder test of Hardy's paradox for $|\Psi\rangle_{3D}$. The empty bars (blue edges) are the Hardy fractions predicted theoretically by Eq. (9), while the solid bars (green) are those obtained experimentally, where $P_1 = 9.23 \pm 0.34\%$, $P_2 = 18.00 \pm 0.54\%$, and $P_3 = 21.85 \pm 0.52\%$. In contrast, all the other 13 joint probabilities are almost zero, in good agreement with the theoretical prediction. Because local realistic models would only allow all probabilities to be zero, the results are nicely demonstrating that quantum mechanics contradicts local hidden variable models.

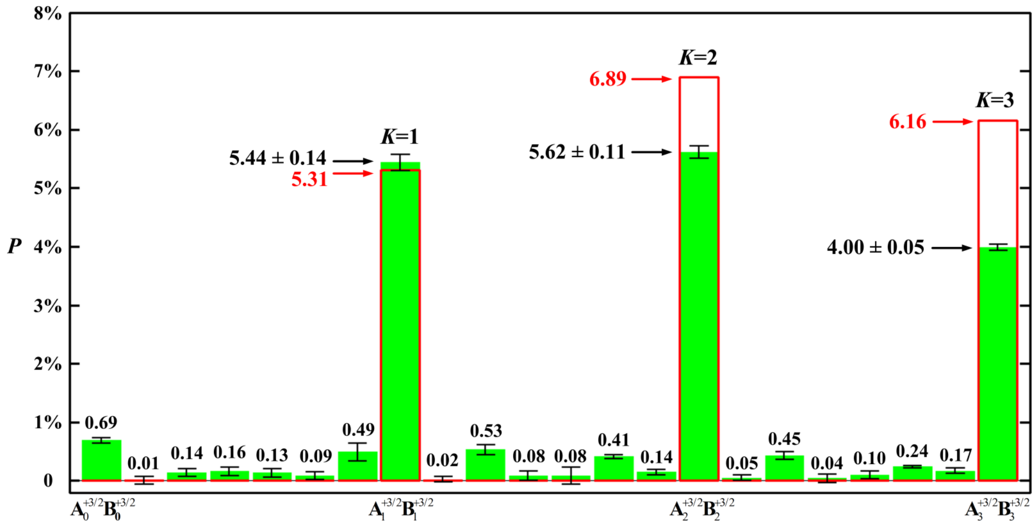

FIG. 4. Experimental results for the ladder test of Hardy's paradox in a four-dimensional OAM subspace. The empty bars (blue edges) are theoretical predictions of the Hardy fractions based on Eq. (13), while the solid bars (green) are those obtained experimentally. The experimental ladder test results in $P_1 = 5.44 \pm 0.14\%$, $P_2 = 5.62 \pm 0.11\%$, and $P_3 = 4.00 \pm 0.05\%$, which is within a good agreement with the theoretical predictions of 5.31, 6.89, and 6.16%. Since all the other 19 joint probabilities are close to zero, our measurements contradict local hidden variable models, which would require zero probabilities for all joint measurements.

mode projections, they are ranging between 0.09 and 0.98%. We experimentally obtain the one-, two-, and three-step Hardy fractions as $P_1 = 9.23 \pm 0.34\%$, $P_2 = 18.00 \pm 0.54\%$, and $P_3 = 21.85 \pm 0.52\%$, respectively. All are well above zero; hence, they clearly contradict the prediction of a local hidden variable model. Additionally, they are close to the quantum-mechanically predicted values, and as such support quantum mechanics. One interesting remark follows: Though the original Hardy fraction p_1 has a bound of $p_H = (5\sqrt{5} - 11)/2 \approx 9\%$ [25], both the theoretical and experimental results in Fig. 3 indicate that our high-dimensional ladder scheme enables the observation of more photon pairs showing contradiction with local realism.

In a second experiment, we extend the ladder test into a four-dimensional OAM subspace, physically equivalent to $s = 3/2$. In order to maximize coincidence counts, we choose the following four-dimensional subspace as the nonmaximally entangled OAM state, $|\Psi\rangle_{4D} = 0.769|0\rangle_A|0\rangle_B + 0.417\,|{+1}\rangle_A|{-1}\rangle_B + 0.414|{-1}\rangle_A|{+1}\rangle_B + 0.251|{+2}\rangle_A|{-2}\rangle_B$. Similar to the three-dimensional experiment, we perform projective measurements on OAM superposition states for both photons (Table S2 of Ref. [38]), and measure the joint probabilities (22 joint measurements in total). The resulting measured probabilities are shown in Fig. 4 together with the theoretical predictions. We find that the one-, two-, and three-step Hardy fractions, $P_1 = 5.44 \pm 0.14\%$, $P_2 = 5.62 \pm 0.11\%$, and $P_3 = 4.00 \pm 0.01\%$, are in good agreement with theoretical values of $P_1 = 5.31\%$, $P_2 = 6.89\%$, and $P_3 = 6.16\%$. All three probabilities are significantly larger than zero in contrast with the other $4Ks + 1 = 19$ joint probabilities, which range from $P_1 = 0.01$ to 0.69%. In theory, these 19 joint probabilities should be exactly zero. However, in our experiment we find small nonzero probabilities, which we attribute to slight misalignment in the optical setup. We thus show again the clear contradiction between quantum mechanics and classical local hidden variable predictions without using inequalities.

V. DISCUSSION AND CONCLUSION

After showing the contraction without using inequalities, it is interesting to investigate the accumulation of errors of our experiment, and test if they allow the drawn conclusions. We do so, in analogy to the two-dimensional cases [40,41], by putting our Hardy paradox in a more general framework in terms of the Clauser-Horne inequality,

$$S_K = \mathrm{P}(A_K = s, B_K = s) - \sum_{k=1}^{K}\sum_{i=-s}^{s-1}[\mathrm{P}(A_k = s, B_{k-1} = i) + \mathrm{P}(A_{k-1} = i, B_k = s)] - \mathrm{P}(A_0 = s, B_0 = s) \leqslant 0, \tag{14}$$

which holds for any local hidden variable theory. For our experimental results, shown in Fig. 3, we find that $S_1 = 6.96 \pm 1.13(\%)$, $S_2 = 14.11 \pm 2.09\%$, and $S_3 = 17.07 \pm 2.69(\%)$. All violate Eq. (14) by more than five standard deviations and, therefore, are evidently contradicting local realism. However, for the data shown in Fig. 4, we only observe a significant violation for the first latter step ($K = 1$), namely, $S_1 = 3.74 \pm 0.69\%$. For the second and third step, we find $S_2 = 2.64 \pm 1.09\%$ and $S_3 = 0.01 \pm 1.35\%$, which is above and around zero due to limited count rates, which results in noise overshadowing the quantum correlations. We further note that the experimentally obtained Hardy fractions in both experiments, $d = 3$ and 4, are deviating from the theoretical values more than the errors bars would suggest. This difference can be attributed to slight misalignments of our optical setup and nonuniformity of the holographic diffraction efficiency. Additionally, higher-dimensional Hardy tests involve more complex OAM superposition states, for which the detection method leads to lower fidelities due to the limited resolution (800×600) of the SLMs used. A possible extension of our paper tackling these challenges would be to prepare optimal Hardy states and manipulate the weights of different OAM states by using suitable filtering processes [42]. Although outside of the scope of this paper, we envision that our experimental scheme could be extended to even higher dimensions by utilizing a brighter source of OAM-entangled photons, and SLMs with a higher resolution.

In conclusion, we have presented an experimental demonstration of a ladder test of Hardy's paradox in a high-dimensional quantum system by using the OAM degree of freedom of photons to mimic spin-s systems. Hardy's paradox can be considered as an example of what Greenberger, Horne, and Zeilinger called "Bell's theorem without inequalities" [43]. Our theoretical formulation and experimental implementation demonstrate that the observation of a single occurrence of an event, here $A_K = s$ and $B_K = s$, suffices to show that quantum mechanics contradicts local realism for high-dimensional quantum systems. We further showed that it is advantageous to use the OAM degree of photons for such a Hardy test: Owing to the limited spiral bandwidth, OAM-entangled photon pairs readily provide a natural set of Hardy's states in high-dimensional Hilbert spaces. Additionally, our observations of the two-step and three-step Hardy tests, shown in Fig. 3, could significantly surpass the one-step Hardy probability bound of $p_H = (5\sqrt{5} - 11)/2$. Recent years have witnessed a rapidly growing interest in high-dimensional quantum entanglement. This paper represents an experiment to demonstrate nonlocality without inequalities for two-photon high-dimensional quantum systems, and may raise interesting possibilities to verify the presence of multiphoton high-dimensional quantum entanglement within the framework of quantum mechanics.

ACKNOWLEDGMENTS

We would like to thank Dr. Jacquiline Romero, Dr. Daniel Giovannini, and Prof. Miles Padgett for kind support and valuable discussions. L.C. acknowledges financial support from the National Natural Science Foundation of China (Grants No. 11474238 and No. 91636109), the Fundamental Research Funds for the Central Universities at Xiamen University (Grant No. 20720160040), the Natural Science Foundation of Fujian Province of China for Distinguished Young Scientists (Grant No. 2015J06002), and the program for New Century Excellent Talents in University of China (Grant No. NCET-13-0495). R.F. acknowledges the support of the Banting postdoctoral fellowship of the Natural Sciences and Engineering Research Council of Canada. E.K. acknowledges the support of the Canada Research Chairs Program.

[1] A. Einstein, B. Podolsky, and N. Rosen, Phys. Rev. **47**, 777 (1935).
[2] J. S. Bell, Physics **1**, 195 (1964).
[3] M. Genovese, Phys. Rep. **413**, 319 (2005).
[4] L. Hardy, Phys. Rev. Lett. **68**, 2981 (1992).
[5] L. Hardy, Phys. Rev. Lett. **71**, 1665 (1993).
[6] N. D. Mermin, Ann. NY Acad. Sci. **755**, 616 (1995).
[7] S. Goldstein, Phys. Rev. Lett. **72**, 1951 (1994).
[8] T. F. Jordan, Phys. Rev. A **50**, 62 (1994).
[9] G. Kar, Phys. Rev. A **56**, 1023 (1997).
[10] G. Di Giuseppe, F. De Martini, and D. Boschi, Phys. Rev. A **56**, 176 (1997).
[11] G. Vallone, I. Gianani, E. B. Inostroza, C. Saavedra, G. Lima, A. Cabello, and P. Mataloni, Phys. Rev. A **83**, 042105 (2011).
[12] L. Chen and J. Romero, Opt. Express **20**, 21687 (2012).
[13] E. Karimi, F. Cardano, M. Maffei, C. de Lisio, L. Marrucci, R. W. Boyd, and E. Santamato, Phys. Rev. A **89**, 032122 (2014).
[14] D. Boschi, S. Branca, F. De Martini, and L. Hardy, Phys. Rev. Lett. **79**, 2755 (1997).
[15] M. Barbieri, F. De Martini, G. Di Nepi, and P. Mataloni, Phys. Lett. A **334**, 23 (2005).
[16] D. Bruß, Phys. Rev. Lett. **81**, 3018 (1998).
[17] H. Bechmann-Pasquinucci and A. Peres, Phys. Rev. Lett. **85**, 3313 (2000).
[18] B. P. Lanyon, M. Barbieri, M. P. Almeida, T. Jennewein, T. C. Ralph, K. J. Resch, G. J. Pryde, J. L. O'Brien, A. Gilchrist, and A. G. White, Nat. Phys. **5**, 134 (2009).
[19] A. Vaziri, G. Weihs, and A. Zeilinger, Phys. Rev. Lett. **89**, 240401 (2002).
[20] A. Dada, J. Leach, G. Buller, M. Padgett, and E. Andersson, Nat. Phys. **7**, 677 (2011).
[21] R. Clifton and P. Niemann, Phys. Lett. A **166**, 177 (1992).
[22] S. Kunkri and S. K. Choudhary, Phys. Rev. A **72**, 022348 (2005).
[23] S. Ghosh and G. Kar, Phys. Lett. A **240**, 191 (1998).
[24] K. P. Seshadreesan and S. Ghosh, J. Phys. A: Math. Theor. **44**, 315305 (2011).
[25] R. Rabelo, L. Y. Zhi, and V. Scarani, Phys. Rev. Lett. **109**, 180401 (2012).
[26] T. Vértesi, S. Pironio, and N. Brunner, Phys. Rev. Lett. **104**, 060401 (2010).
[27] A. Cabello, Phys. Rev. A **58**, 1687 (1998).
[28] G. Molina-Terriza, J. P. Torres, and L. Torner, Nat. Phys. **3**, 305 (2007).
[29] A. M. Yao and M. J. Padgett, Adv. Opt. Photon. **3**, 161 (2011).
[30] P. M. Rios and E. Straume, *Symbol Correspondences for Spin Systems* (Springer, Berlin, 2014).
[31] L. Allen, M. W. Beijersbergen, R. J. C. Spreeuw, and J. P. Woerdman, Phys. Rev. A **45**, 8185 (1992).
[32] G. Molina-Terriza, J. P. Torres, and L. Torner, Phys. Rev. Lett. **88**, 013601 (2001).
[33] A. Forbes, A. Dudley, and M. McLaren, Adv. Opt. Photon. **8**, 200 (2016).
[34] J. P. Torres, A. Alexandrescu, and L. Torner, Phys. Rev. A **68**, 050301 (2003).
[35] A. Yariv and P. Yeh, *Optical Waves in Crystals* (Wiley, New York, 1983).
[36] M. Born and E. Wolf, *Principle of Optics* (Cambridge University, Cambridge, England, 1997).
[37] A. Mair, A. Vaziri, G. Weihs, and A. Zeilinger, Nature (London) **412**, 313 (2001).

[38] See Supplemental Material at http://link.aps.org/supplemental/10.1103/PhysRevA.96.022115 for tables of joint OAM projections, the SLM configurations, the high-order unitary matrices, and proof of Eq. (14).
[39] A. M. Yao, New J. Phys. **13**, 053048 (2011).
[40] N. D. Mermin, Am. J. Phys. **62**, 880 (1994).
[41] A. Garuccio, Phys. Rev. A **52**, 2535 (1995).
[42] A. Vaziri, J. W. Pan, T. Jennewein, G. Weihs, and A. Zeilinger, Phys. Rev. Lett. **91**, 227902 (2003).
[43] D. M. Greenberger, M. A. Horne, A. Shimony, and A. Zeilinger, Am. J. Phys. **58**, 1131 (1990).